Sensors & Transducers, Vol. 196, Issue 1, January 2016, pp. 82-87

Sensors & Transducers

http://www.sensorsportal.com

Research of an Optoelectronic Current Transformer Based on a Designed Magneto-Optic Sensor

[1, *] R. El-Bashar, [1] J. El-Azab, [1] Y. Badr and [2] R. Yousif

[1] National Institute of Laser Enhanced Sciences, Cairo University, Egypt

[2] Electrical Power and Machines Department, Faculty of Engineering, Cairo University, Egypt

[*] Tel.: 201064088409

[*] E-mail: r.albashar@niles.edu.eg

Received: 2 January 2016 /Accepted: 25 January 2016 /Published: 30 January 2016

Abstract: An Optical Current Transformer (OCT) with dual polarimetric configuration is evaluated using a magneto-sensitive glass SF-59 of 0.4 and 1.3 cm lengths located into an air gapped TCT iron core. Using a 5 mW He-Ne laser light source at 632.8 nm, the maximum current measured is nearly 2800 A with maximum error of 0.6 % and 1 % for the two sensors lengths 0.4 and 1.3 cm, respectively. The results have been experimentally limited the maximum output of Variac. The simulation of the electronic circuit of the current transducer is introduced and the results indicated the reliability and accuracy of using the OCT in measurement and protection.

Keywords: Verdet constant, Optical current transformer, Optical current sensor, Bulk glass.

1. Introduction

Due to the recent demand of power consumption and expansions of electric power system network, a great number of protection zones become exist requiring intelligent system. Current sensors are important devices as they are not only give the accurate power consumption but also used for the fast detection and identification of failures points in power systems. However, Traditional Current Transformers (TCT) have enormous limitations due to their saturation problems, huge size and weight, high insulation cost as well the sensitivity to electromagnetic interference (EMI) [1].

Recently, optoelectronic technology is one of the evolved solutions of TCT problems by converting the TCT output voltage into a corresponding frequency modulated optical signal. This signal is not influenced by EMI and is congruous with intelligent network of current measurement and protection. However, this technology could not overcome the iron core saturation [2]. The development of the measurement circuit of Rogowski coil sensor which does not involve iron core, for high current measurement is still in progress [3]. On the other hand, magneto-optic sensing method provided an alternate solution for solving the TCT problems [4]. It consumes less power as compared to the traditional Dc Hall Effect sensor used in plants such as Aluminum factories [5]. OCT can be integrated with fiber-optic based Ethernet local area networks. Besides, replacing the traditional solution which digitizes the TCT output for relays, meters, and SCADA systems [6].

The effect of the magnetic field on the transmission of light through certain transparent optical material was first observed by Michael Faraday in 1845 [7]. He noticed that, when the transmitted linearly polarized light is subjected to a magnetic field B in the direction

of propagation, the plane of polarization rotates. Based on this effect, optical current sensors were developed into mainly two types; bulk glass sensors and fiber optical sensors. In bulk sensors, an optical material sensitive to the magnetic field is positioned parallel to the lines of magnetic field induced by a conductor carrying the current to be sensed. This sensor has the advantages of small size, low cost, weak influence of the environmental conditions such as temperature, pressure and other noises and high sensitivity to magnetic field. The sensitivity of the sensor is directly proportional to the length of the material subjected to the magnetic field. To increase its sensitivity, the sensor was designed to surround the conductor. The geometrical structure promotes the propagation of light parallel to the magnetic field lines. It can be either rectangular or triangular and sometimes circular [7-9]. In this case, the sensitivity is based on the sensor structure and/or the multiple path of light within the optical material [10].

While in optical fiber sensors, the bulk glass is replaced by an optical fiber with a large number of turns around the conductor in analogy with TCT where the magnetic field cut a number of turns wound around its core. The closed circular optical path of light within the optical fiber provides the immunity from electromagnetic interference. However, its high linear birefringence increases the influence of the environmental conditions on the sensor performance, and its Verdet constant is less than the bulk glass [7].

An alternative technique is to utilize a small bulk sensor which does not surround the conductor while compensating the reduced sensor length by using a material with a high Verdet constant [11-13] and a concentrator core to increase the magnetic field [14-16].

In this work, an evaluation of a dual quadrature Polarimetric sensitive optical current sensor inserted into a gapped iron core is carried out. In Section 2, the design of the optical current sensor (OCS) in a gapped iron core will be introduced. The proposed electronic circuit of the OCT will be presented in Section 3. The simulation of the electronic Circuit and optical sensor experimental results are introduced in Section 4 and will be concluded in Section 5.

2. OCS System Design

2.1. Optical Current Sensor

The Schematic diagram and equivalent circuit of optical sensor are shown in Fig. 1. The system consists of a Toroid core with an air gap which causes a magnetic drop in the magnetic circuit. In the equivalent circuit, the core and the gap are represented by $\mathcal{R}_c$ and $\mathcal{R}_g$, respectively [17].

According to Ampere's circuital law, the Ampere-turns (Ni) is given by:

$$Ni = \phi_c \mathcal{R}_{c+} \phi_g \mathcal{R}_g, \quad (1)$$

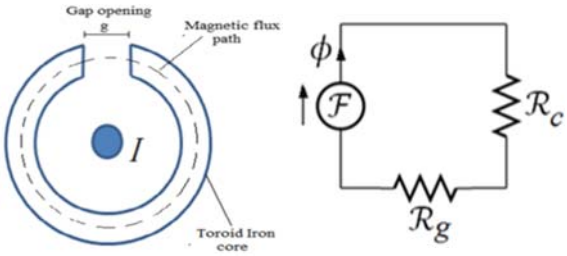

(a) (b)

Fig. 1. (a) Toroid core with an air gap and (b) its electric representation circuit.

$$Ni = \phi_c \frac{l_c}{\mu_c A_c} + \phi_g \frac{l_g}{\mu_g A_g}, \quad (2)$$

where ϕ_i is the flux, l_i is the mean length, A_i is the cross section area where the flux pass through, and μ_i is the permeability. And the subscript i (= c and g) represents the core and the gap, respectively. The air gap permeability μ_g nearly equals the free space permeability $\mu_0 = 4\pi 10^{-7} \mathrm{T.m/A}$. For the core permeability $\mu_c = \mu_0 \mu_{cr}$, where μ_{cr} is the relative permeability of the core. By neglecting the flux lines that are diffused outside the common area of the core and the air gap, then $A_c = A_g = A$. Considering core flux ϕ_c and the gap flux ϕ_g are equal, the Ampere-turns becomes

$$NI = \frac{\phi}{A}\left(\frac{l_c}{\mu_c} + \frac{l_g}{\mu_0}\right) \quad (3)$$

The magnetic flux density becomes:

$$B = NI \frac{1}{\left(\frac{l_c}{\mu_c} + \frac{l_g}{\mu_0}\right)} \quad (4)$$

2.2. Polarimetric Detection OCS Setup [9-10]

A dual Polarimetric schematic setup [17-18] is presented in Fig. 2. It consists from a He-Ne laser source (5 mW, 632.8 nm), a polarizer, polarizing beam splitter (PBS) and two photo detectors connected to an oscilloscope. The Toroid iron core with an appropriate number of turns is used to generate a magnetic flux corresponding to that the flux resulting from the power line conductor current.

The rotation in the polarization plane depends on the intensity of magnetic field B, the length of interacting material d, and the Verdet constant V, representing the medium sensitivity to magnetic field, through the following relation [7].

$$\theta = BVd \quad (5)$$

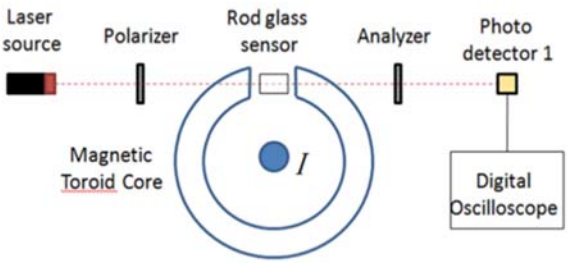

Fig. 2. The Dual quadrature Polarimetric schematic setup.

Through Mauls's law, the output from the PBS (P_o) is given by

$$P_0=P_1\cos^2(\phi), \quad (6)$$

where ϕ is the angle between transmission axes of the polarizer and the PBS, P_1 is the power transmitted from the polarizer. The sensor sensitivity is optimized by adjusting the polarizer transmission angle to 45 degree with respect to the PBS. In the absence of the magnetic field (i.e. no electric current applied), the angle ϕ between polarizer and PBS remains 45°. The angle of rotation for the two outputs is altered in the presence of magnetic field to be:

$$\phi = 45 \pm \theta,$$

where θ is the angle of Faraday rotation. Thus, the light power outputs from the PBS falling on the detectors become:

$$P_{o1} = \frac{1}{2}P_1 + \frac{1}{2}P_1\, sin(2\theta) \quad (7)$$

$$P_{o2} = \frac{1}{2}P_1 - \frac{1}{2}P_1\, sin(2\theta) \quad (8)$$

The two optical detectors convert the optical signal into electrical signal where the subtraction and addition are executed electronically. By dividing the two components (subtraction and addition) by an electronic divider, the resulting signal is proportional to the applied current. The division of these components also removes the effect of the light power fluctuation [9]. The output signal of the electronic divider becomes:

$$S = \frac{P_{o1}-P_{o2}}{P_{o1}+P_{o2}}$$

And for small angles,

$$S = sin(2\theta) \approx 2\theta \quad (9)$$

In case of alternating currents, the output signal can be expressed by:

$$S = 8\pi 10^{-7} Ni \frac{1}{(\frac{l_c}{\mu_{cr}} + l_g)} Vd\ sin\omega t \quad (10)$$

3. The Proposed Electronic Circuit of the OCT

The schematic diagram of the electronic circuit of OCT is shown in Fig. 3. It represents the electronic processing of the detected signals as discussed in Section 2.B in order to obtain a signal proper for metering and relaying circuits.

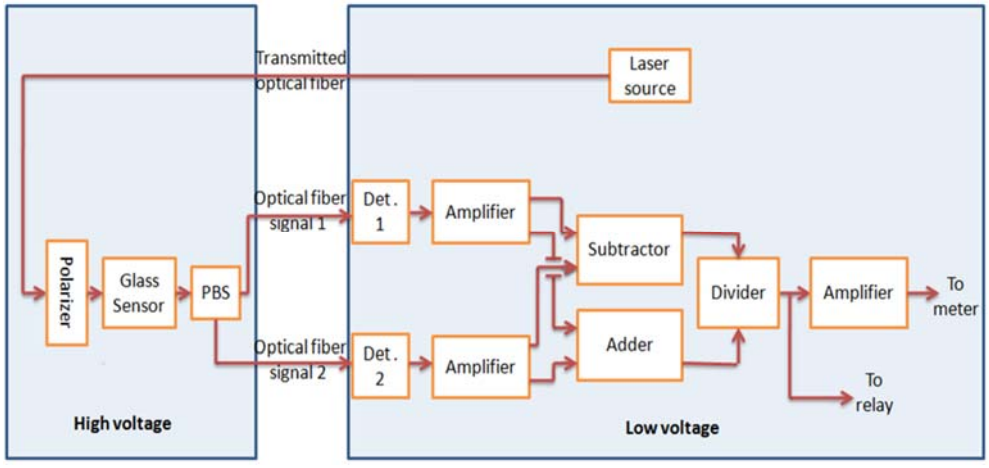

Fig. 3. Schematic block diagram of the proposed optical current transformer**.**

Fig. 4 introduces the equivalent circuit of the amplifier namely transimpedance amplifier. The reversed bias is used to convert the photodetected current Ip into Vout controlled by the resistor Rf. The circuit output is generated and simulated on the simulator program as an input to the proposed electronic circuit [19].

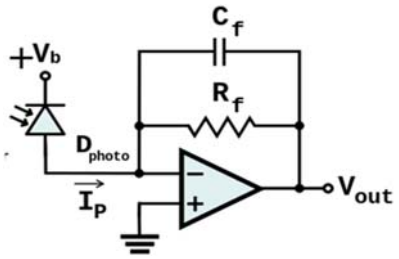

Fig. 4. The Transimpedance amplifier circuit.

The simulation of the electronic circuit is illustrated in details in Fig. 5, showing the amplifier, subtractor [20], adder, and divider [21]. The subtractor removes of the dc component and increases the current signal sensitivity. The adder circuit is used to get the dc component of the detected signal. The divider plays the main job to extract the electric signal corresponding to the measured current. Finally, the resulting signal is amplified for current measurements systems.

4. Simulation and Experimental Results

4.1. Measurement circuit Simulation

The simulation of the electronic circuit is carried out by Proteus 8. In Fig. 6, Ch. (A) is the optical signal which equal 0.315 V, as adjusted experimentally, with noise fluctuations 4 % at 1.5 kHz and 2 % at 15 kHz. The simulation parameters of the OCS are as following; the Verdet constant V = 25.9 rad/T.m for SF-59 glass [22], glass length d=1.3 cm. For a current 1500 A, the magnetic flux density is measured experimentally to be 119 mT. At this values, the AC signal is simulated from Equation (9) to be equal 0.08 V in amplitude (maximum value) at 50 Hz. The outputs of transimpedance amplifier circuits of the two detectors are Ch. (B) and Ch. (C) while the output of the adder, subtractor, and divider are shown in Fig. 7 as well as the output of the amplified current signal for the metering system.

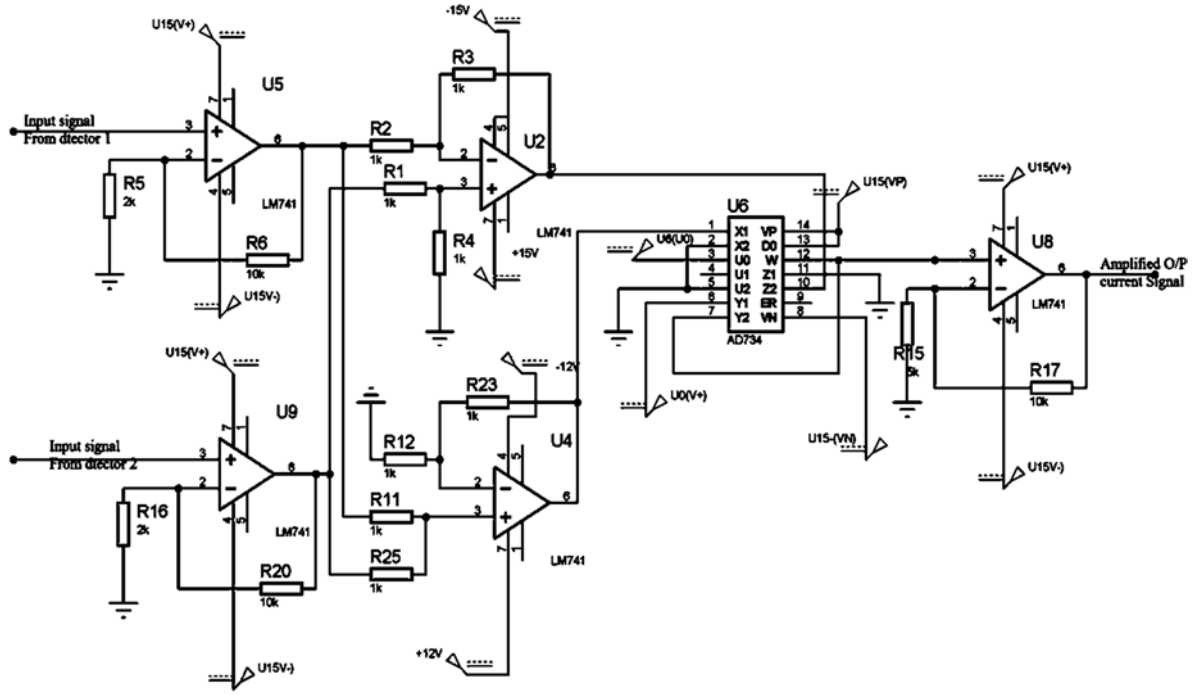

Fig. 5. The proposed electronic circuit.

4.2. Experimental Results of OCS

Experimentally, the conductor current is simulated by wounding the air gapped iron core by an appropriate number of turns in order to obtain an equivalent magnetic field in the gap. As a result, the gap magnetic field becomes a function of the product of the winding current and the turns number. The optical sensor behavior is studied experimentally by using 5 mW He-Ne laser light at 632.8 nm wavelength with attenuator OD3. The Toroid iron core coil is supplied from the Variac to control the applied current. A Gauss / Tesla Meter model 4048 with T-4048-001 Probe from F.W. Bell model is used. Fig. 8 shows the relation between the magnetic field in the center of the gap and the applied current. The output signals from the two detectors are displayed on HEWLETT PAKWARD HP 54503A – 500 MHz digitizing oscilloscope. The peak to peak voltage difference output signal of the two detectors is shown in Fig. 9 as a function with ampere-turns for the two sensor lengths 0.4 and 1.3 cm.

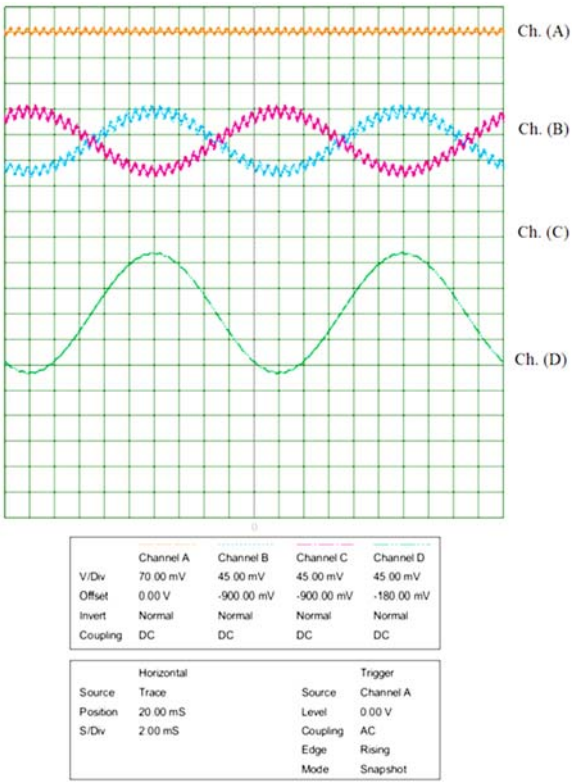

Fig. 6. Oscilloscope output - Ch. (A): light signal, Ch. (B): detector 1 signal, Ch. (C): detector 2 signal and Ch. (D): Subtractor O/P signal.

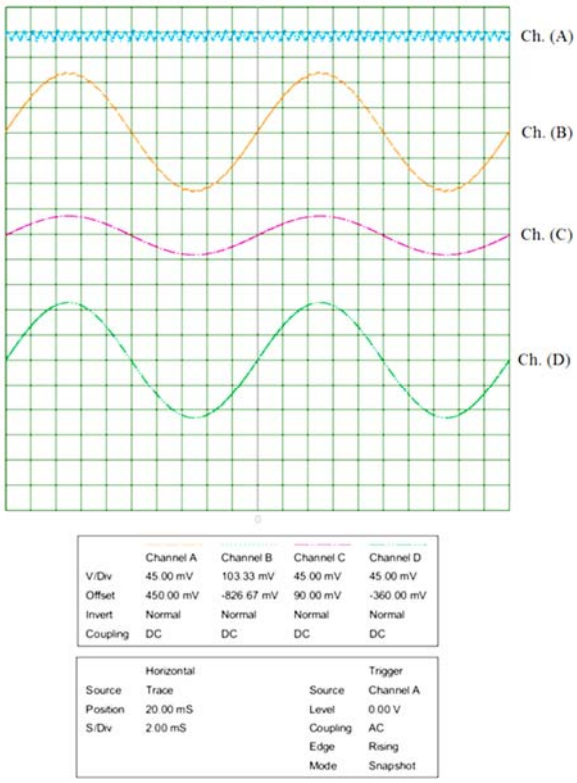

Fig. 7. Oscilloscope output - Ch. (A): Adder O/P signal, Ch. (B): Subtractor O/P signal, Ch. (C): Divider O/P current signal and Ch. (D): Amplified current signal.

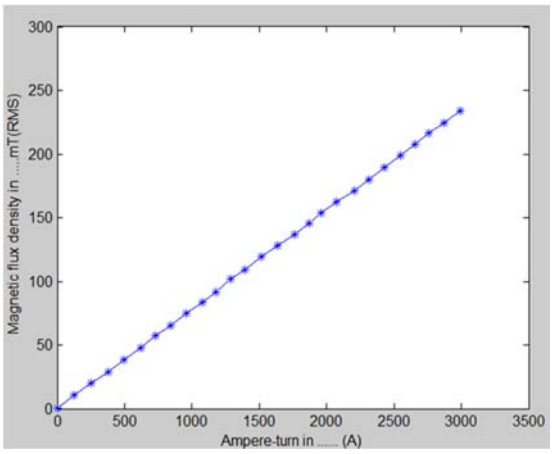

Fig. 8. The Ampere-turn versus the magnetic field in the gap center of the Toroid iron core.

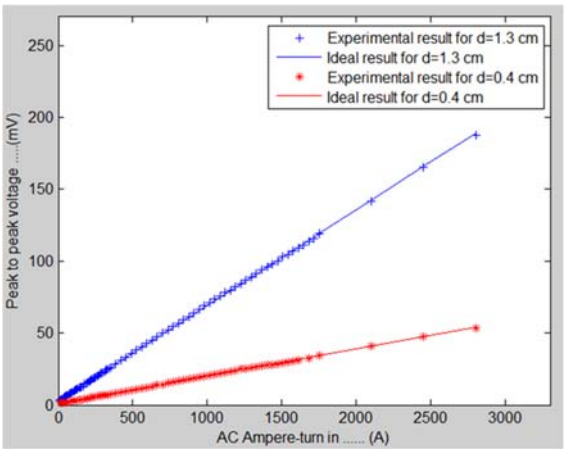

Fig. 9. The Peak to peak output voltage as a function of the applied AC current ($I=Ni$) in the cases of d=0.4 and 1.3 cm.

The experimental results showed a good agreement with the calculations. The long glass length (1.3 cm) provided better results as the light passing through the glass effectively interacts with the magnetic field in the gap and the sensitivity of the sensor is higher. However, the calculated R.M.S error of the long length is higher than the short length as it changes from 0.42 and 0.27. Thus, a trade-off between the strength of the obtained signal and the corresponding error is obtained and the selection will be user-defined.

5. Conclusions

This work presented an evaluation of an optical current transformer for high voltage network using a magneto-sensitive SCHOTT glass SF-59 inserted into a gapped core of a TCT. The OCS results were carried out experimentally while the validity of the sensor was verified numerically. The experiment was realized by using a 5 mW He-Ne laser at 632.8 nm for a two glass sensors of lengths 0.4 and 1.3 cm. Using a dual

quadrature polarimetric configuration, the obtained results showed that the sensitivity of the sensor is dependent on the sensor length with a trade-off with the R.M.S error. Therefore, it can be concluded that the optical current transformer can be utilized as a high sensitive sensor for high voltage networks.

Acknowledgements

The authors gratefully acknowledge Mr. Wahed Morsi for his collaboration in cutting and polishing the glass.

References

[1]. Brigida A. C. S., Nascimento I. M., Mendonça S., Costa J. C. W. A., Martinez M. A. G., Baptista J. M., Jorge P. A. S., Experimental and theoretical analysis of an optical current sensor for high power systems, *Photonic Sensors*, Vol. 3, No. 1, 2013, pp. 26-34.

[2]. Popescu M., Manta A., Păduraru N., Marinescu A., Optoelectronic current transformer for medium voltage networks, *Annals of the University of Craiova, Electrical Engineering Series*, No. 34, 2010, pp. 103-108.

[3]. Bing Y., Yutian W., Hui L., Huixin W., Yiqiang C., Research of Measurement Circuits for High Voltage Current Transformer Based on Rogowski Coils, *Sensors & Transducers*, Vol. 165, Issue 2, February 2014, pp. 35-39.

[4]. Barczak K., Optical fibre current sensor for electrical power engineering, *Bulletin of the Polish Academy of Sciences. Technical Sciences*, Vol. 59, No. 4, 2011, pp. 409-414.

[5]. Bohnert K., Brändle H., Brunzel M. G., Gabus P., Guggenbach P., Highly accurate fiber-optic DC current sensor for the electrowinning industry, *IEEE Transactions on Industry Applications*, Vol. 43, No. 1, 2007, pp. 180-187.

[6]. Skendzic V., Ender I., Zweigle G., IEC 61850-9-2 process bus and its impact on power system protection and control reliability, in *Proceedings of the 9th Annual Western Power Delivery Automation Conference*, Spokane, WA, April 2007.

[7]. Silva R. M., Martins H., Nascimento I., Baptista J. M., Ribeiro A. L., Santos J. L., Frazão O., Optical Current Sensors for High Power Systems: A Review, *Appl. Sci.*, No. 2, 2012, pp. 602-628.

[8]. Sato T., Takahashi G., Inui Y., Method and apparatus for optically measuring a current, Washington, DC: U.S. Patent and Trademark Office, U.S. Patent No. US 4564754 A, 1986.

[9]. Fisher N. E., Jackson D. A., Vibration immunity and Ampere's circuital law for a near perfect triangular Faraday current sensor, *Measurement Science and Technology*, Vol. 7, No. 8, 1996, pp. 1099-1102.

[10]. Ning Y. N., Chu B. C. B., Jackson D. A., Miniature Faraday current sensor based on multiple critical angle reflections in a bulk-optic ring, *Optics Letters*, Vol. 16, Issue 24, 1991, pp. 1996-1998.

[11]. Chen Q., Chen Q., Wang S., A new Faraday rotation measurement method for the study on magneto optical property of PbO-Bi2O3-B2O3 glasses for current sensor applications, *Open Journal of Inorganic Non-metallic Materials*, Vol. 1 No. 1, 2011, pp. 1-7.

[12]. Westenberger G., Hoffmann H. J., Jochs W. W., Przybilla G., Verdet constant and its dispersion in optical glasses, *Proceedings SPIE*, Vol. 1535, November 1991, pp. 113-120.

[13]. Malak S., Suzuki I. S., Suzuki M. S., Faraday rotation measurement using a lock-in amplifier, 2011, https://www.researchgate.net/publication/269929805_Faraday_rotation_measurement_using_a_lock-in_amplifier

[14]. Mihailovic P., Petricevic S., Stojkovic Z., Radunovic J. B., Development of a portable fiber-optic current sensor for power systems monitoring, *IEEE Transactions on Instrumentation and Measurement*, Vol. 53, No.1, 2004, pp. 24-30.

[15]. Li G., Kong M. G., Jones G. R., Spencer J. W., Sensitivity improvement of an optical current sensor with enhanced Faraday rotation, *Journal of Lightwave Technology*, Vol. 15, No. 12, 1997, pp. 2246-2252.

[16]. Yi B., Chu B. C. B., Chiang K. S., Chung H. S., New design of optical electric-current sensor for sensitivity improvement, *IEEE Transactions on Instrumentation and Measurement,* Vol. 49, No. 2, 2000, pp. 418-423.

[17]. Wang S., Karri A., Harlev Y., Use of dual-frequency excitation method to improve the accuracy of an optical current sensor, *Proceedings SPIE, Photonic Fiber and Crystal Devices: Advances in Materials and Innovations in Device Applications,* Vol. 7420, August 2009.

[18]. Katsukawa H., Ishikawa H., Okajima H., Cease T. W., Development of an optical current transducer with a bulk type Faraday sensor for metering, *IEEE Transactions on Power Delivery*, Vol. 11, No. 2, 1996, pp. 702-707.

[19]. Photo diode Transimpedance Amplifier circuit, http://repository.asu.edu/attachments/56952/content/LaFevre_asu_0010N_10920.pdf

[20]. Operational amplifier - Available online: http://www.electronics-tutorials.ws/opamp/opamp_5.html

[21]. Lorsawatsiri A., Kiranon W., Silaruam V., Sangpisit W., Wardkein P., Simple and Accurate Frequency to Voltage Converter, in *Proceedings of the International Conference on Electrical Engineering/Electronics Computer Telecommunications and Information Technology (ECTI-CON),* 2010, pp. 212-215.

[22]. Weber M. J., Handbook of optical materials, Laser and Optical Science and Technology Series, *CRC Press.* 2002.